J Sol-Gel Sci Technol (2010) 53:287–292
DOI 10.1007/s10971-009-2089-9

ORIGINAL PAPER

Aerosol-assisted synthesis of mesoporous titania nanoparticles with high surface area and controllable phase composition

Zhiwang Wu · Yunfeng Lu

Received: 2 September 2009 / Accepted: 3 October 2009 / Published online: 15 October 2009

Abstract Mesoporous titania nanoparticles (denoted as MTN) with high surface area (e.g., 252 $m^2 g^{-1}$) were prepared using tetrapropyl orthotitanate (TPOT) as a titania precursor and 10–20 nm or 20–30 nm silica colloids as templates. Co-assembly of TPOT and silica colloids in an aerosol-assisted process and immediate calcination at 450 °C resulted in anatase/silica composite nanoparticles. Subsequent removal of the silica colloids from the composite by NaOH solution created mesopores in the TiO_2 nanoparticles with pore size corresponding to that of silica colloids. Effects of silica colloids' contents on MTN porosity and crystallites' growth at a higher calcination temperature (e.g., 1000 °C) were investigated. Silica colloids suppressed the growth of TiO_2 crystallites during calcination at a higher calcination temperature and controllable contents of the silica colloids in precursor solution resulted in various atomic ratios of anatase to rutile in the calcinated materials. The mesostructure and crystalline structure of these titania materials were characterized by transmission electron microscope (TEM), scanning electron microscope (SEM), X-ray diffraction (XRD), differential thermal analysis (DTA)-thermo-gravimetric analysis (TGA), and N_2 sorption.

Z. Wu (✉) · Y. Lu
Department of Chemical and Biomolecular Engineering, Tulane University, New Orleans, LA 70118, USA
e-mail: zhiwang.wu@gmail.com

Y. Lu (✉)
Department of Chemical and Biomolecular Engineering, University of California Los Angeles, Los Angeles, CA 90095, USA
e-mail: luucla@ucla.edu

Keywords Titania · Mesoporous · Nanoparticles · Sol–gel · Aerosol · Self-assembly · Phase transition

1 Introduction

Mesoporous titania materials have attracted much interest over the past decades because of their properties such as chemical stability, high surface area, high pore volume, controllable pore size, phase composition, and morphology, which make mesoporous titania the potential candidates for gas sensors, photocatalysts for degrading organic pollutants in water, photoelectrodes for photosplitting water, solar energy conversion, and Li ion battery materials [1–10]. Mesoporous materials are usually synthesized by sol–gel reaction using surfactant as reaction template [11–16] and the wall of the synthesized materials is normally amorphous. Crystallization of these materials under heat treatment or UV light irradiation could easily destroy the three-dimensional mesostructure and reduce the photocatalytic activity because it is hard for the thin wall to retain the structure during phase transformation from amorphous to crystalline framework. To avoid the collapse of the mesostructure, several methods as follows have been taken to prepare mesoporous titania materials with a crystalline wall. Depositing materials on the inner surface of the titania mesoporous wall can strengthen the thin wall of the titania materials and results in mesoporous titania with crystalline wall after crystallization [17]. Or, direct synthesis of crystalline mesoporous titania without above-mentioned supporting agent can be achieved by controlling the crystallization speed and deposition of very tiny titania crystallites on the surface of surfactant molecular assemblies. Removal of the surfactant by solvent extraction at room temperature could result in the mesoporous titania

with crystalline wall. For example, hydrothermal treatment method [18] using CTAB as the surfactant has been applied to synthesize the crystalline mesoporous titania.

In this work, colloidal silica nanoparticles were used to replace the traditional nanoscale molecular assemblies (e.g., surfactant) since colloidal silica particles were stable at the titania crystalline temperature (e.g., ca. 450 °C) and could stabilize the thin wall of the MTN material during its transformation from amorphous to crystalline phase. Easy removal of the colloidal silica template by 3.5 M NaOH solution at low temperature (e.g., 80 °C) resulted in crystalline titania particles with replicated mesopores from the colloidal silica template. Materials calcined at 450 °C resulted in the anatase titania which is one of the three titania polymorphs (i.e., anatase, rutile, and brookite) and the anatase titania usually exhibits the highest photocatalytic activity among the three polymorphs [8, 18]. Aerosol-assisted process was used for the self-assembly of titania precursor and colloidal silica into nanocomposite.

Calcination at higher temperature (e.g., 600–1000 °C) [19] usually transforms the titania polymorphs from anatase to rutile. The titania materials synthesized using colloidal silica as a template, however, disobeyed the tendency of the transformation. Contrarily, mixture of anatase and rutile or even pure anatase could be achieved at a calcination temperature of 1000 °C and ratio of anatase to rutile could be easily adjusted by changing amounts of colloidal silica added into the sol–gel precursor mixture.

2 Experimental

The MTN material was synthesized by an aerosol-assisted sol–gel process and details about the sol–gel process were described in our previous papers [20–22]. In a typical synthesis of the MTN, HCl (37%, Aldrich) solution was firstly added into absolute ethanol and tetrapropyl orthotitanate (TPOT, Aldrich), 10–20 nm colloidal silica (ST-N, Nissan chemical) or 20–30 nm colloidal silica (ST-O, Nissan chemical) were added into the acidic solution in sequence. The molar ratio of TPOT: colloidal silica: ethanol: HCl: H_2O was 1:(0.6–2.4):48:0.55:1.9. The molar ratio of Si/Ti (i.e., colloidal silica/TPOT) varied from 0.6 to 2.4 to control final MTN porosity as well as ratio of anatase to rutile upon calcination at a temperature of 1000 °C. The aerosol reactor used a commercial atomizer (Model 3076, TSI, Inc., St Paul, MN) operated with nitrogen as a carrier/atomization gas at a volumetric flow rate of 2.6 LSTP min^{-1}, in which the N_2 flow was laminar (Reynolds number was 75 at 400 °C). Confined spherical droplets experienced ~3 s of drying at RT and ~3 s of heating at 400 °C in a tubular reactor(~110 cm in length, ~1 inch in diameter), resulting in spherical TiO_2/(colloidal silica) composite naoparticles collected on a filter maintained at 80 °C. In general, such atomizer produces polydispersed particles from a few tens to hundreds of nanometers. The amorphous composite was then calcinated at 450 °C for 3 h in air with a heating rate of 1 °C/min to fully crystallize the TiO_2. The as-synthesized composite was also calcinated at 1000 °C for 3 h in the air with a heating rate of 5 °C/min to study the colloidal silica's effect on the ratio of anatase to rutile. Colloidal silica was then completely removed (confirmed by EDX analysis not shown here) from the titania/(colloidal silica) composite nanoparticles by soaking the composites in a 3.5 M NaOH solution at 80 °C for 48 h under continuous stirring, resulting in the MTN material with high crystallinity.

Powder X-ray diffraction (XRD) patterns were recorded on a Siemens D500 diffractometer operated at 40 kV, 30 mA (Cu-Kα radiation, $\lambda = 0.15406$ nm). N_2 adsorption–desorption isotherms were measured at 77 K on a Micromeritics ASAP 2010 analyzer. The mesopore size distribution was calculated from the desorption isotherms using Barrett-Joyner-Halenda (BJH) algorithm. Transmission electron microscopy (TEM) images were taken using a JEOL 2010 microscope operated at 200 kV. Field emission scanning electron microscopy (FE-SEM) images were obtained using a Hitachi S-4800 microscope. Materials were mounted using a conductive carbon double-sided sticky tape. Differential thermal analysis (DTA)-Thermogravimetric analysis (TGA) pattern was obtained from a Thermal Analysis SDT 2960 instrument with a heating rate of 10 °C min^{-1} in air.

3 Results and discussion

3.1 Mesoporous titania nanoparticles with high surface area

Figure 1a shows a typical transmission electron microscopy (TEM) image of the as-synthesized amorphous titania/(colloidal silica) composite nanoparticles by the aerosol-assisted process. The composite particles are almost spherical except that there are some protruding silica colloids on the surface (as indicated by black arrows). Figure 1b, c shows the typical TEM images of the MTN after the crystallization at 450 °C and the removal of colloidal silica template by NaOH. A lot of 20–30 nm pores replicated from colloidal silica can be observed in these nanoparticles. Electron diffraction (ED) pattern (inset, Fig. 1b) confirms the highly crystalline structure of the MTN.

Figure 2 shows the nitrogen adsorption–desorption isotherms and the Barrett-Joyner-Halenda (BJH) pore size

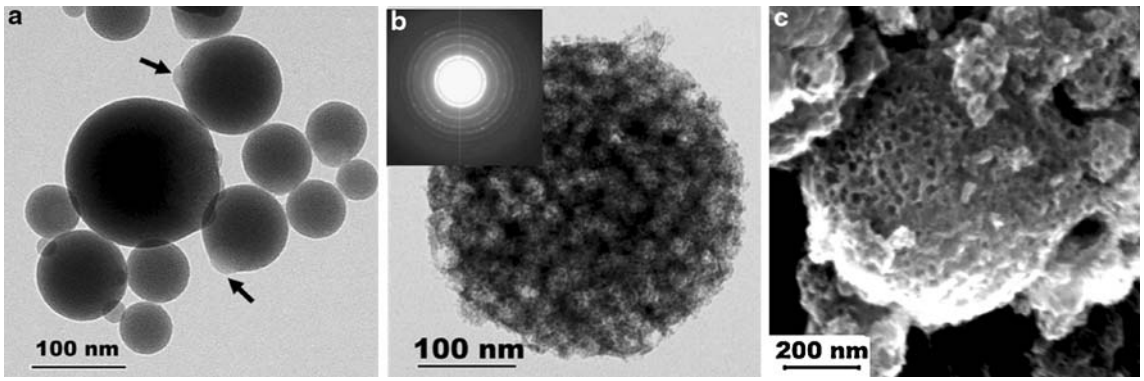

Fig. 1 **a** TEM image of the as-synthesized amorphous titania/(colloidal silica) composite, **b** TEM image, ED pattern (*inset b*), and **c** FESEM image of the MTN after titania crystallization and removal of the colloidal silica. All the samples are prepared by using 20–30 nm colloidal silica as templates with Si/Ti = 1.2

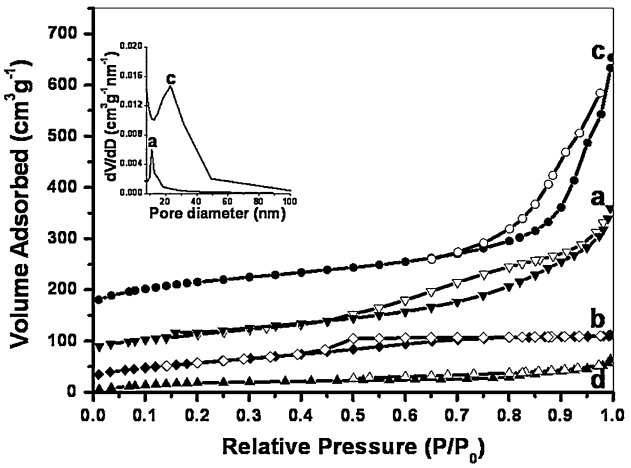

Fig. 2 Nitrogen adsorption–desorption isotherms and BJH pore size distributions (*inset*) of the mesoporous titania prepared by using colloidal silica as templates: *a* 10–20 nm colloidal silica, Si/Ti = 1.2; *b* 10–20 nm colloidal silica, Si/Ti = 1.8; *c* 20–30 nm colloidal silica, Si/Ti = 1.2; *d* 20–30 nm colloidal silica, Si/Ti = 1.8. To allow a better clarity, curve a and curve c were shifted up by 50 and 150 $cm^3\ g^{-1}$, respectively

distributions (insets) of the MTN (Fig. 2a–d) templated with different Si/Ti molar ratio and its physicochemical properties are correspondingly listed in Table 1. For the MTN synthesized using 10–20 nm colloidal silica as templates (Fig. 2a, b), increase of Si/Ti molar ratio from 1.2 (Fig. 2a) to 1.8 (Fig. 2b) resulted in decreased surface area (from 252 to 210 $m^2\ g^{-1}$) and pore volume (from 0.39 to 0.17 $cm^3\ g^{-1}$). The same trend was observed for 20–30 nm colloidal silica template (Fig. 2c, d), which has a decreased surface area from 251 to 79 $m^2\ g^{-1}$ and pore volume from 0.61 to 0.08 $cm^3\ g^{-1}$ with an increase of Si/Ti molar ratio from 1.2 (Fig. 2c) to 1.8 (Fig. 2d). The decreased surface areas and pore volumes were attributed to collapse of the mesostructure formed at the Si/Ti ratio of 1.2 (confirmed by TEM images, not shown here). MTN synthesized with smaller Si/Ti ratio than 1.2 was also measured (not shown here) but both surface area and pore volume were not as high as with the Si/Ti ratio of 1.2. That is, Si/Ti molar ratio for a highest surface area was around 1.2 but the ratio as big as 1.8 led to the collapse of the mesostructure. According to IUPAC recommendations [23], type of hysteresis loops shown in Fig. 2a, c is intermediate between H1 (at $0.45 < P/P_0 < 0.7$ for Fig. 2a and $0.7 < P/P_0 < 0.9$ for Fig. 2c) and H3 (at $0.7 < P/P_0 < 1.0$ for Fig. 2a and $0.9 < P/P_0 < 1.0$ for Fig. 2c). The H1 loops indicated there are relatively centralized pore sizes inside the MTN (see Fig. 1c) from the colloidal silica template, while the H_3 loops up to $P/P_0 \approx 1.0$ reflect the existence of interparticles pores. Pore size distribution curves (insets) agree well with the colloidal silica templates (i.e., 10–20 nm for curve a and 20–30 nm for curve c).

Figure 3 shows the XRD patterns of the MTN prepared using 10–20 nm colloidal silica (Fig. 3a) or 20–30 nm colloidal silica (Fig. 3b) as templates. Both of the patterns have typical anatase peaks (JCPDS No. 21-1272) irrespective of colloidal silica's amounts or sizes. Since a certain amount of our particles are greater than 100 nm (Fig. 1) and have sizes ranging from tens to hundreds of nanometers, Schërrer equation is not applicable in calculation of the mean particle size.

A typical TGA-DTA pattern of the as-synthesized amorphous titania/(colloidal silica) composite by aerosol process is shown in Fig. 4. At temperatures below 120 °C, the water which have been condensed and adsorbed in the material evaporates, which led to an endothermic peak (as indicated by a black arrow). An exothermic peak (as indicated) of the DTA curve at ca. 415 °C is assigned to the crystallization of amorphous titania. That is, crystallization of titania took place in the range of 120–415 °C and completed at 415 °C which is the reason why 450 °C was chosen for the crystallization of the as-synthesized titania/(colloidal silica) composite.

Table 1 Physicochemical properties of titania materials prepared with or without colloidal silica as templates at a calcination temperature of 450 °C

Sample code	Templates	Si/Ti (molar ratio)	Surface area (m^2 g^{-1})	Pore volume (cm^3 g^{-1})	Pore diameter (nm)
–	–	0	16	0.03	8.1
a	10–20 nm colloidal silica	1.2	252	0.39	6.3
b		1.8	210	0.17	3.2
c	20–30 nm colloidal silica	1.2	251	0.61	6.7
d		1.8	79	0.08	6.0

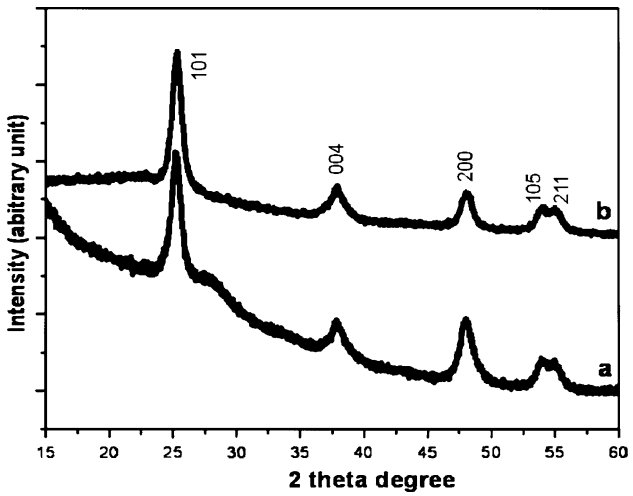

Fig. 3 High-angle XRD patterns of the mesoporous titania prepared using colloidal silica as templates: *a* 10–20 nm colloidal silica, Si/Ti = 1.2; ***b*** 20–30 nm colloidal silica, Si/Ti = 1.2

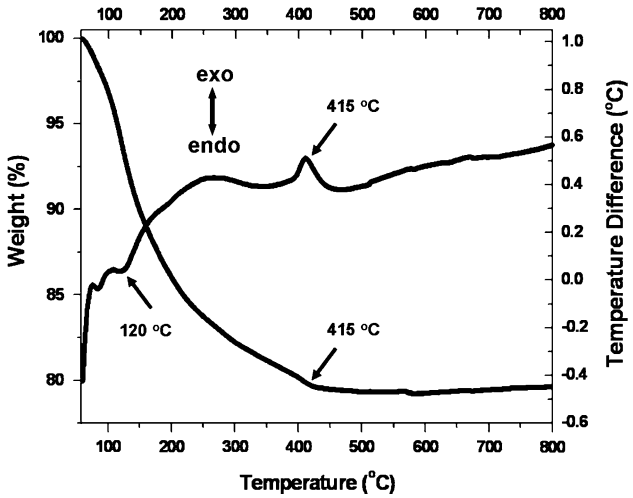

Fig. 4 TGA-DTA pattern in air of the as-synthesized amorphous titania/(colloidal silica) composite

3.2 Effects of colloidal silica on crystalline structure of mesoporous titania

Figure 5 shows typical transmission electron microscopy (TEM) images of the MTN materials prepared using a calcination temperature of 1000 °C in the air instead of 450 °C. Without colloidal silica template, titania nanoparticles (Fig. 5a) fused together upon calcination at 1000 °C. Contrarily, the MTN material (Fig. 5b) prepared with a Si/Ti molar ratio of 2.4 remained its spherical shape after calcination at 1000 °C. 10–20 nm colloidal silica templates can also be observed in Fig. 5b (darker area).

Figure 6 shows the XRD patterns of the MTN materials prepared without (Fig. 6a) or with various amounts of colloidal silica template (Fig. 6b, c, d). Titania material synthesized without any colloidal silica template (Fig. 6a) exhibits only rutile peaks (JCPDS No. 21-1276) while incorporation of 10–20 nm colloidal silica template into titania materials led to weaker rutile peaks (Fig. 6b, c) than Fig. 6a with certain anatase peaks and anatase peaks are getting stronger with the increase of Si/Ti molar ratio from 0 (Fig. 6a) to 0.6 (Fig. 6b) and 1.2 (Fig. 6c). Further increase of Si/Ti molar ratio to 2.4 (Fig. 6d) results in pure anatase titania (JCPDS No. 21-1272). The percentage of the anatase phase was calculated as listed in Table 2 by the formula [24] $C_a = [1 + 1.26(I_r/I_a)]^{-1}$, where C_a is the anatase percentage, I_r and I_a are the intensities of peaks (110) of rutile and peaks (101) of anatase, respectively. As shown in Table 2, increase of Si/Ti molar ratio from 0 to 2.4 significantly decreased the rutile percentage from 100 to 0. Growth of titania crystallites without the colloidal silica completely turned anatase into rutile while the calcination temperature rose from 450 to 1000 °C at a rate of 5 °C/min. Presence of colloidal silica in the titania phase significantly decreased the surface energy of the titania phase and completely retarded growth of titania crystallites from anatase to rutile with the Si/Ti molar ratio of 2.4.

Figure 7 shows the nitrogen adsorption–desorption isotherms and the BJH pore size distribution (inset) of the MTN materials prepared without (Fig. 7a) or with (Fig. 7b, c, d) 10–20 nm colloidal silica templates. All the detailed physicochemical properties of the corresponding materials and Degussa P25 are listed in Table 2. As discussed in Fig. 5a, titania particles prepared without template is almost dense with a negligible surface area of 4 m^2 g^{-1}, and pore volume of 0.01 cm^3 g^{-1}. Surface area of the MTN materials (samples b–d) can even reach as high as

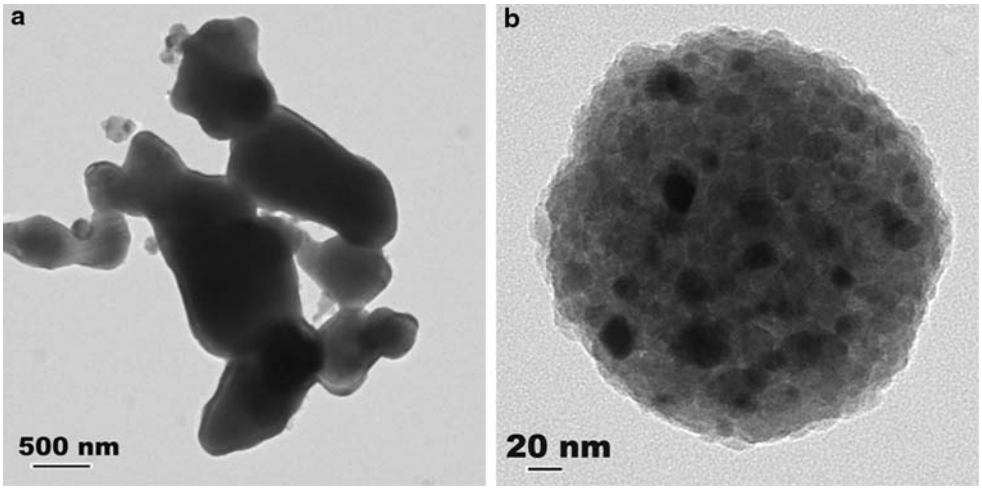

Fig. 5 TEM images of the MTN materials prepared **a** without, **b** with 10–20 nm colloidal silica as template (Si/Ti = 2.4)

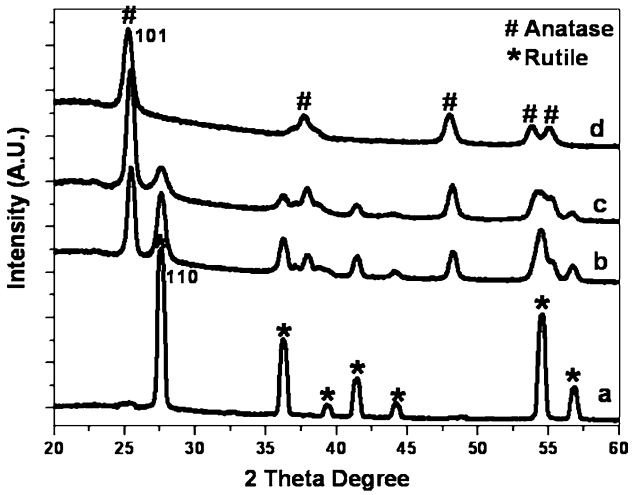

Fig. 6 High-angle XRD patterns of the MTN materials prepared *a* without, *b–d* with 10–20 nm colloidal silica as template: *b* Si/Ti = 0.6; *c* Si/Ti = 1.2; and *d* Si/Ti = 2.4

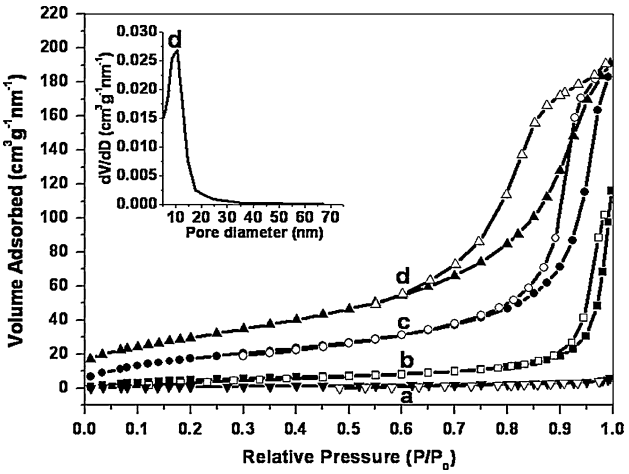

Fig. 7 Nitrogen adsorption–desorption isotherms and BJH pore size distributions (*inset*) of the mesoporous titania after the removal of colloidal silica from the 1000 °C calcinated titania materials prepared *a* without, *b–d* with 10–20 nm colloidal silica as template: *b* Si/Ti = 0.6; *c* Si/Ti = 1.2; and *d* Si/Ti = 2.4

109 m^2 g^{-1} (sample d) which is twice that of commercially used P25 (55 m^2 g^{-1}). Surface area as large as possible and an appropriate anatase content of 80% (P25) was believed to have the best photocatalytic activity [25]. Among all the prepared samples, sample c has the most similar anatase content (81.6%) while it has higher surface area and pore volume than P25. Figure 7b, c, d have a similar type of hysteresis loops as the samples discussed previously in

Table 2 Physicochemical properties of titania materials prepared with or without colloidal silica as templates at a calcination temperature of 1000 °C

Sample code	Templates	Si/Ti (molar ratio)	Surface area (m^2 g^{-1})	Pore volume (cm^3 g^{-1})	Anatase content (%)	Rutile content (%)
P25	–	–	55	0.12	80	20
a	–	0	4	0.01	0	100
b	10–20 nm colloidal silica	0.6	21	0.07	52.4	47.6
c		1.2	69	0.25	81.6	18.4
d		2.4	109	0.28	100	0

Fig. 2. Pore size distribution curve (inset) corresponds well to the 10–20 nm colloidal silica template.

4 Conclusions

Mesoporous anatase or anatase/rutile titania nanoparticles with surface area as high as 252 m^2 g^{-1} have been successfully synthesized by an aerosol-assisted sol–gel process. Comparisons have been conducted with respect to the Si/Ti molar ratio and calcination temperature. An appropriate Si/Ti ratio can result in high surface area while excessive colloidal silica content can lead to the collapse of mesostructure. Anatase/rutile titania can only be obtained with a high calcination temperature (e.g., 1000 °C) using colloidal silica templates. Anatase contents are controllable in anatase/rutile titania by adjusting the Si/Ti ratio in precursor solution. Higher content of colloidal silica helps to retard the growth of titania crystallites and results in higher percentage of anatase.

Acknowledgments The authors gratefully acknowledge the financial support of this work by NASA (Grant No. NAG-1-02070 and NCC-3-946), the Office of Naval Research, the Louisiana Board of Regents (Grant No. LEQSF(2001-04)-RD-B-09), National Science Foundation (Grant No. NSF-DMR-0124765, and CAREER award).

References

1. Khan SUM, Shahry MA, Ingler WB (2002) Science 297:2243
2. Stiehl JD, Kim TS, McClure SM, Mullins CB (2004) J Am Chem Soc 126:13574
3. Yu JC, Zhang LC, Yu JG (2002) Chem Mater 14:4647
4. Cabrera S, El-Haskouri J, Beltran-Portier A, Beltran-Portier D, Marcos AD, Amoros P (2000) Solid State Sci 2:513
5. Wagemaker M, Kentgens APM, Mulder FM (2002) Nature 418:397
6. Chen MS, Goodman DW (2004) Science 306:252
7. Gao XP, Zhu HY, Pan GL, Ye SH, Lan Y, Wu F, Song DY (2004) J Phys Chem B 108:2868
8. Ovenstone J, Yanagisawa K (1999) Chem Mater 11:2770
9. Kavan L, Kalbac M, Zukalova M, Exnar I, Lorenzen V, Nesper R, Graetzel M (2004) Chem Mater 16:477
10. Stone VF, Davis RJ (1998) Chem Mater 10:1468
11. Kresge CT, Leonowicz ME, Roth WJ, Vartuli JC, Beck JS (1992) Nature 359:710
12. Attard GS, Glyde JC, Goltner CG (1995) Nature 378:366
13. Davis SA, Burkett SL, Mendelson NH, Mann S (1997) Nature 385:420
14. Huo Q, Leon R, Petroff PM, Stucky GD (1995) Science 268:1324
15. Li D, Zhou H, Honma I (2004) Nat Mater 3:65
16. Miyata H, Suzuki T, Fukuoka A, Sawada T, Watanabe M, Noma T, Takada K, Mukaide T, Kuroda K (2004) Nat Mater 3:651
17. Shibata H, Ogura T, Mukai T, Ohkubo T, Sakai H, Abe M (2005) J Am Chem Soc 127:16396
18. Peng T, Zhao D, Dai K, Shi W, Hirao K (2005) J Phys Chem B 109:4947
19. Liu H, Yang W, Ma Y, Ye X, Yao J (2003) New J Chem 27:529
20. Wu ZW, Hu QY, Pang JB, Jakobsen HP, Yu DH, Lu YF (2005) Microporous Mesoporous Mater 85:305
21. Hampsey JE, Hu Q, Wu Z, Rice L, Pang J, Lu Y (2005) Carbon 43:2977
22. Hampsey JE, Hu Q, Rice L, Pang J, Wu Z, Lu Y (2005) Chem Commun 28:3606
23. Gregg SJ, Sing KSW (1982) Adsorption, surface area and porosity, 2nd edn. Academic Press, London
24. Huang W, Tang X, Wang Y, Koltypin Y, Gedanken A (2000) Chem Commun 1415
25. Kasuga T, Hiramatsu M, Hoson A, Sekino T, Niihara K (1998) Langmuir 14:3160